Timing Is Everything: Highly Specific and Transient Expression of a MAP Kinase Determines Auxin-Induced Leaf Venation Patterns in *Arabidopsis*

Vera Stanko[a,b], Concetta Giuliani[a,c], Katarzyna Retzer[a,d], Armin Djamei[a,e], Vanessa Wahl[f], Bernhard Wurzinger[g,h], Cathal Wilson[a,i], Erwin Heberle-Bors[a], Markus Teige[g,j,1], and Friedrich Kragler[f,g,1]

a Department of Plant Molecular Biology, Max. F. Perutz Laboratories, University of Vienna, Dr. Bohrgasse 9/4, Vienna, A-1030, Austria
b Present address: Felix-Klein-Gymnasium, Böttingerstraße 17, D-37073 Göttingen, Germany
c Present address: Austrian Centre of Industrial Biotechnology, Muthgasse 11, A-1190 Vienna, Austria
d Present address: Department of Applied Genetics and Cell Biology, University of Natural Resources and Life Sciences, Muthgasse 18, A-1190 Vienna, Austria
e Present address: Gregor Mendel Institute of Molecular Plant Biology, Dr. Bohr-Gasse 3, 1030 Vienna, Austria
f Max Planck Institute of Molecular Plant Physiology, Wissenschaftspark Golm, Am Mühlenberg 1, D-14476 Potsdam-Golm, Germany
g Department of Biochemistry, Max. F. Perutz Laboratories, University of Vienna, Dr. Bohrgasse 9/5, Vienna, A-1030, Austria
h Present address: Department of Ecogenomics and Systems Biology, University of Vienna, Althanstr. 14, A-1090 Vienna, Austria
i Present address: Telethon Institute of Genetics and Medicine, Via Pietro Castellino, 111, 80131-Naples, Italy
j Department of Ecogenomics and Systems Biology, University of Vienna, Althanstr. 14, A-1090 Vienna, Austria

ABSTRACT **Mitogen-activated protein kinase (MAPK) cascades are universal signal transduction modules present in all eukaryotes. In plants, MAPK cascades were shown to regulate cell division, developmental processes, stress responses, and hormone pathways. The subgroup A of *Arabidopsis* MAPKs consists of AtMPK3, AtMPK6, and AtMPK10. AtMPK3 and AtMPK6 are activated by their upstream MAP kinase kinases (MKKs) AtMKK4 and AtMKK5 in response to biotic and abiotic stress. In addition, they were identified as key regulators of stomatal development and patterning. *AtMPK10* has long been considered as a pseudo-gene, derived from a gene duplication of *AtMPK6*. Here we show that *AtMPK10* is expressed highly but very transiently in seedlings and at sites of local auxin maxima leaves. *MPK10* encodes a functional kinase and interacts with the upstream MAP kinase kinase (MAPKK) AtMKK2. *mpk10* mutants are delayed in flowering in long-day conditions and in continuous light. Moreover, cotyledons of *mpk10* and *mkk2* mutants have reduced vein complexity, which can be reversed by inhibiting polar auxin transport (PAT). Auxin does not affect *AtMPK10* expression while treatment with the PAT inhibitor HFCA extends the expression in leaves and reverses the *mpk10* mutant phenotype. These results suggest that the AtMKK2–AtMPK10 MAPK module regulates venation complexity by altering PAT efficiency.**

Key words: ***Arabidopsis*** MAP kinase; leaf development; polar auxin transport; leaf venation pattern.

Stanko V., Giuliania C., Retzera K., Djamei A., Wahl V., Wurzinger B., Wilsona C., Heberle-Bors E., Teige M., and Kraglerf F. (2014). Timing is everything: highly specific and transient expression of a MAP Kinase determines auxin-induced leaf venation patterns in arabidopsis. Mol. Plant. 7, 1637–1652.

[1] To whom correspondence should be addressed. M.T. E-mail markus.teige@univie.ac.at, fax +43-1-4277-876551, tel. + 43-1-4277-76530. F.K. E-mail kragler@mpimp-golm.mpg.de, fax +49-331-567-8100, tel. 49-331-567 8120.

doi:10.1093/mp/ssu080 Advance Access publication 26 July 2014
Received 26 February 2014; accepted 4 July 2014

INTRODUCTION

Mitogen-activated protein kinase (MAPK) signaling pathways are key regulators of cell proliferation, differentiation, and stress responses (Colcombet and Hirt, 2008; Andreasson and Ellis, 2010; Rodriguez et al., 2010). The core of the MAP kinase signal transduction cascade is composed of a three-kinase module consisting of a MAP kinase kinase kinase (MAPKKK), a MAP kinase kinase (MAPKK), and a MAP-activated protein kinase (MAPK). Upon cellular stimulation, specific serine/threonine MAPKKKs are activated, leading to phosphorylation and activation of a subset of downstream MAPKKs, which in turn activate MAPKs at a conserved TXY phosphorylation motif. Since their initial discovery in plants (Duerr et al., 1993; Jonak et al., 1993), functional analysis on plant MAP kinases has mainly been focused on their role in different stress responses, and only a few studies reported on their role in plant development (Wilson et al., 1997; Bogre et al., 1999; Nishihama et al., 2001). However, since the discovery that stomatal development is regulated by a MAP kinase cascade (Bergmann et al., 2004; Lukowitz et al., 2004), the central role of plant MAP kinases as regulators of developmental processes came into focus again (Lampard et al., 2009; Meng et al., 2012).

In *Arabidopsis*, the MAPK family consists of more than 60 MAPKKK, 10 MAPKK, and 20 MAPK genes (Group, 2002). *Arabidopsis* MAPKs are clustered into four groups named A to D. The smallest group A includes the three members AtMPK3, AtMPK6, and AtMPK10 (Hamel et al., 2006). AtMPK3 and AtMPK6 are activated by biotic elicitors such as flagellin via AtMKK4/5 (Asai et al., 2002), or by oxidative stress (Rentel et al., 2004). AtMPK4 and AtMPK6, and their upstream MAPKK AtMKK2, are activated by abiotic stresses such as high salinity and cold (Ichimura et al., 2000; Teige et al., 2004). In addition to their well-established role in regulation of plant stress response, analysis of mutant plants inferred also a function of *AtMPK3* and *AtMPK6* in developmental decisions in the embryo, anther, and inflorescence, and for regular stomatal distribution on the leaf surface (Bergmann et al., 2004; Gray and Hetherington, 2004; Bush and Krysan, 2007) such as by phosphorylation of the basic helix–loop–helix (bHLH) transcription factor SPEECHLESS (Lampard et al., 2008). The embryo-lethal phenotype observed in *atmpk3/atmpk6* double-knockout plants indicates that AtMPK3 and AtMPK6 are at least partially redundant (Wang et al., 2007). The broad role of these MAPKs in the regulation of a wide array of cellular functions is underlined by the identification of many different substrates of AtMPK6 and AtMPK3 in large-scale proteomic approaches (Feilner et al., 2005; Popescu et al., 2009).

Functional links between hormone- and MAPK signaling have been found for different hormones and MAPK modules (Kovtun et al., 1998; Cardinale et al., 2002; Dai et al., 2006; Takahashi et al., 2007; Khan et al., 2013). For example, AtMPK3 and AtMPK6 are activated by abscisic acid (ABA) treatment. In the ABA-hypersensitive hyl1-mutant, transcripts of AtMPK3 and its upstream MAPKKK ANP1 are up-regulated and ANP1 is repressed upon ABA treatment (Lu et al., 2002). In addition, ANP1 has been proposed to act upstream of AtMPK3 and AtMPK6 inducing expression of stress-responsive genes and transcriptional repression of auxin inducible genes (Kovtun et al., 1998, 2000). Thus, this kinase cascade seems to link oxidative stress responses to the regulatory function of the growth hormone auxin.

The plant hormone auxin plays a crucial role in vascular differentiation. Auxin synthesis and degradation and auxin distribution control vascular differentiation and consequently also patterning (Sachs, 2000). In plants, the vascular system is composed of xylem and phloem and extends throughout the whole plant body. Dicotyledonous plants are characterized by a reticulated venation of leaves. Vein formation starts at the margin of young leaves and proceeds inside the leaf by the conversion of files of procambial cells into vascular bundles. Secondary veins branch towards the margins from both sides of the central midvein and extend acropetally towards the tip. Additional veins branch from the midvein and the secondary veins creating tertiary and quaternary veins or open ends (Candela et al., 1999).

The auxin signal flow canalization hypothesis proposes that, in developing leaves, auxin first diffuses from the site of biosynthesis at the margins and eventually induces the formation of a polar auxin transport (PAT) system. In turn, this event enhances auxin transport and leads to a canalization of auxin flow along a file of procambial cells that progressively differentiate into vascular bundles (Sachs, 1991). Regulated auxin flow requires symmetrically localized influx and efflux carriers on the plasma membrane (Marchant et al., 1999; Steinmann et al., 1999; Swarup et al., 2001). Auxin also seems to move acropetally through the epidermis into meristems in apices to regulate the formation of leaf primordia (Reinhardt et al., 2000; Avsian-Kretchmer et al., 2002).

Synthetic PAT inhibitors like 1-naphthylphthalamic acid (NPA) or 9-hydroxyfluorene-9-carboxylic acid (HFCA) have been used in several studies to investigate the role of auxin distribution in vascular development. External application of PAT inhibitors leads to an array of aberrant developmental phenotypes including incorrect embryonic axis formation (Liu et al., 1993; Ruegger et al., 1997; Hadfi et al., 1998; Sabatini et al., 1999; Kerk et al., 2000), delayed hypocotyl and root elongation in light (Jensen et al., 1998), and altered vascular patterning (Mattsson et al., 1999).

The activity of auxin transport proteins seems also to be controlled by reversible protein phosphorylation. The broad-spectrum kinase inhibitors staurosporine and K252a rapidly reduce auxin efflux, suggesting that protein phosphorylation may be essential to sustain the

activity of the efflux carrier (Delbarre et al., 1998). In particular, tyrosine kinase inhibitors, likely to affect tyrosine phosphorylation of MAPKs, were found to reduce auxin efflux (Bernasconi, 1996). Based on the altered vascular patterns and auxin distribution in *bud1* mutant plants, in which the MAPKK AtMKK7 was overexpressed, Dai et al. (2006) suggested that MAPK cascades have the potential to enhance PAT.

In contrast to *AtMPK6* and *AtMPK3*, the third member of *Arabidopsis* group A kinases, *AtMPK10*, shows very low transcriptional activity according to RT–PCR (Miles et al., 2005) and microarray assays (Hamel et al., 2006). It was therefore proposed that *AtMPK10* constitutes a non-functional pseudo-gene generated by a segmental duplication of the closely related group A member *AtMPK6* (Hamel et al., 2006). Here, we demonstrate that AtMPK10 displays kinase activity, is expressed in a very narrow time window early in leaf development in limited areas of leaves, and interacts specifically with the upstream MAPKK AtMKK2 previously shown to mediate stress resistance (Teige et al., 2004). Under long-day conditions, *atmpk10* mutants are delayed in bolting and flowering. Plants lacking AtMKK2 or AtMPK10 activity have a simpler venation pattern, while plants overexpressing AtMPK10 have the opposite phenotype. PAT inhibitors were able to reverse the altered venation pattern of *atmkk2* or *atmpk10* mutants. From these data, we propose a model where the AtMKK2/AtMPK10 signaling module operates in *Arabidopsis* as a regulator of auxin transport responsible for vein patterning.

RESULTS

AtMPK10 Is Active in Leaves

Initially, *AtMPK10* has been assumed to be a pseudo-gene with low or no transcriptional activity and redundant function in the MAPK cascade (Hamel et al., 2006). Thus, we addressed the potential *AtMPK10* function by characterizing its transcriptional activity *in planta*. The predicted 700-bp-long *AtMPK10 promoter* region was cloned into a glucuronidase (GUS) reporter binary vector to generate transgenic lines. Eight independent transgenic lines were isolated and analyzed by histochemical GUS enzyme activity assays starting from 1-day-old seedlings to 28-day-old plants (Figure 1A–1I). No GUS activity could be detected 1 d after germination (DAG) (Figure 1A). GUS activity was observed in the tips of the cotyledons at 2 DAG and, from 4 to 12 DAG, the signal appeared at the margins of cotyledons and in a patchy manner along their veins (Figure 1B and 1C). In 12- to 28-day old plants, GUS staining was found to coincide with small regions of minor veins, the marginal vasculature, the leaf tips, and the tips of the serrated margin of rosette leaves where veins meet (Figure 1D–1I). The latter sites represent hydathodes (water-exporting glands). To further support the observed *AtMPK10* expression, we performed RT–PCR assays on seedlings. As with GUS assays, we detected high *AtMPK10* mRNA signals 2 DAG, which decreased 4 DAG and remained very low at later stages (Figure 1J). During embryogenesis, consistently with online available expression data (Winter et al., 2007), *AtMPK10* expression seems to be restricted to the globular stage and was extremely low in RNA *in situ* assays (see Supplementary Data).

Isolation and Molecular Characterization of an *AtMPK10* Mutant Line

To perform a functional analysis, we identified an *atmpk10* T-DNA insertion mutant line in the SALK collection (#N539102). Southern blot analysis indicated that the SALK line carries a T-DNA insertion at a single site. As shown in Figure 1K, three T-DNA elements inserted in a tandem-repeat rearrangement were identified leading to silencing of the Kanamycin resistance gene present in the T-DNA insertion. PCR and sequencing analyses revealed that the T-DNA insertion occurred in the first exon of the gene, 160 base pairs after the predicted start codon. The insertion line did not produce detectable amounts of *AtMPK10* RNA. Thus, we had isolated a single insertion *atmpk10* null-mutant that was then used for further characterization.

AtMPK10 Shows Kinase Activity

In order to test whether the predicted protein possesses MAP kinase activity, we produced a GST-fusion protein of the wild-type and two mutant versions of AtMPK10 in *Escherichia coli* and tested them with myelin basic protein (MBP) as substrates in *in vitro* kinase assays (Figure 2A). The AtMPK10 AEF mutant was created by changing the conserved Threonine and Tyrosine residues of the TEY MAPK phosphorylation motif in the activation loop to Alanine ($T_{218}A$) and to Phenylalanine ($Y_{220}F$), respectively. The R89 mutant was created by changing one of the two conserved Lysine residues (88 and 89) of the ATP-binding loop to an Arginine ($K_{89}R$). The wild-type AtMPK10 showed phosphorylation activity similar to the well-characterized group B MAPK AtMPK4, whereas no auto-phosphorylation activity and a strongly reduced substrate phosphorylation almost to background levels was detected with the AtMPK10 AEF version. In contrast, the exchange of only one of the two Lysine residues of the ATP-binding domain was not sufficient to abolish MPK10 kinase activity (R89). Thus, the predicted AtMPK10 exhibits kinase activity that depends on a functional phosphorylation motif and we considered the AEF version of MPK10 as a loss-of-function (LOF) version and used this in the further experiments.

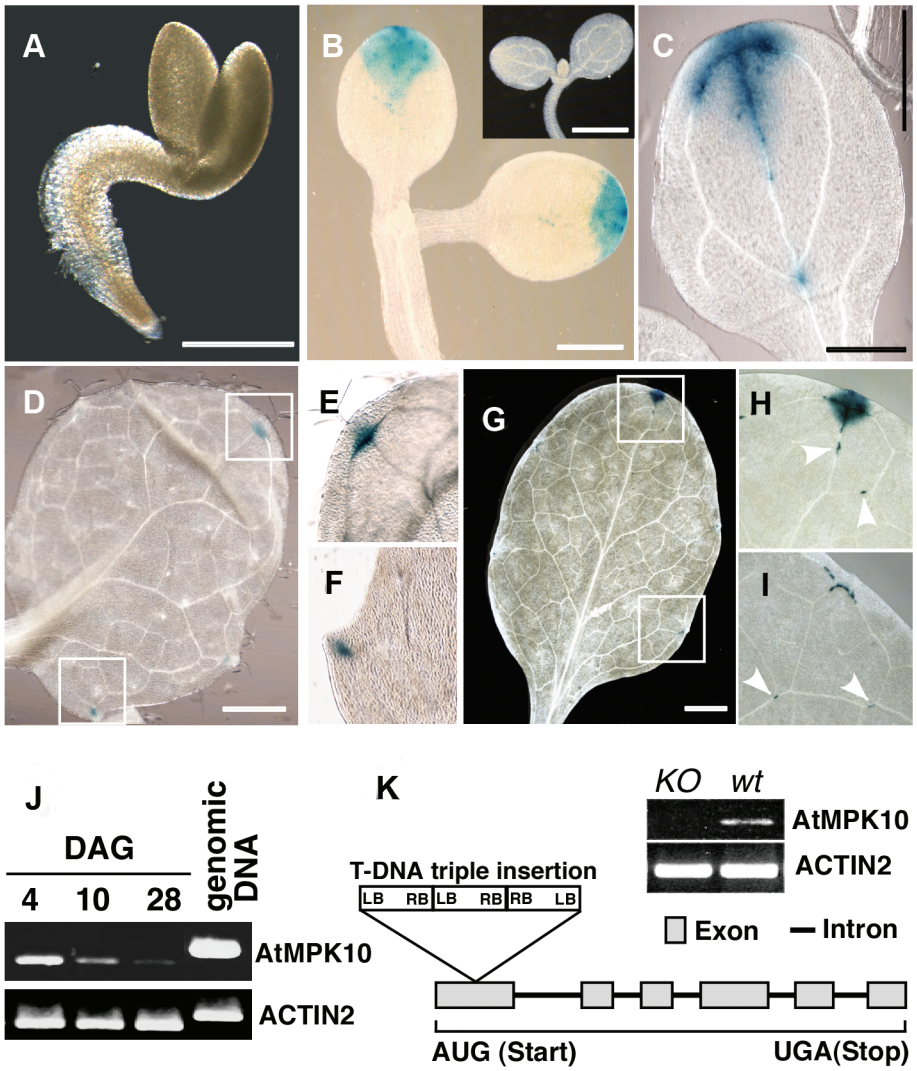

Figure 1 *AtMPK10* Expression Profile and Molecular Characterization of *atmpk10* Mutant Plants.

(A–I) Histochemical localization of GUS activity of *Pro*$_{AtMPK10}$*::GUS* plants. (A) 1 days after germination (DAG) no promoter activity is detected. (B) 4 DAG seedlings demonstrate strong promoter activity in the tips of cotyledons. Insert shows a wild-type control plant submitted to GUS staining. (C) 12 DAG the promoter is active in cotyledons but rather restricted to the vasculature. (D–F) The first true leaves show a GUS signal restricted to the leaf tip (E), and at the tips of the serrated margin (F). (G–I) 28 DAG GUS is detected in the leaf tip (G, H) and marginal regions of the leaf (I). Note additional signals at the connections of minor veins of the lamina (arrow heads). Bar = 1 mm.

(J) RT–PCR analysis of Col-0 wild-type seedlings RNA. A high signal of *AtMPK10* 4 DAG decreased at 10 DAG and 28 DAG. Note that the control with *ACTIN2*-specific primers resulted in an equal signal at all stages.

(K) Identification of an *atmpk10* mutant SALK line. The T-DNA insertion, consisting of a tandem-repeat rearrangement of three T-DNA elements, is present at 160 bp after the ATG in the predicted first exon of *AtMPK10*. RT–PCR analysis on homozygous *atmpk10* KO mutants confirmed the absence of *AtMPK10* mRNA in this line. *ACTIN2*-specific RT–PCR served as a positive control.

AtMPK10 Interacts Specifically with the Upstream MKK AtMKK2

To identify potential upstream MAP kinase kinase interaction partner(s) of AtMPK10, we employed the yeast two-hybrid interaction system. All 10 known *Arabidopsis* MKKs were fused to the GAL4 binding domain and confirmed to mediate no auto-activation of the β-galactosidase (β-GAL) reporter system. In the presence of AtMPK10, only AtMKK2 but not the other nine MAPKKs triggered activation of the two-hybrid system (Figure 2B). This indicated that AtMPK10 interacts specifically with AtMKK2 and no other upstream *Arabidopsis* MKK.

Next we used RT–PCR assays to ask whether *AtMKK2* and *AtMPK10* have an overlapping expression profile and could function together at the same time. As presented in

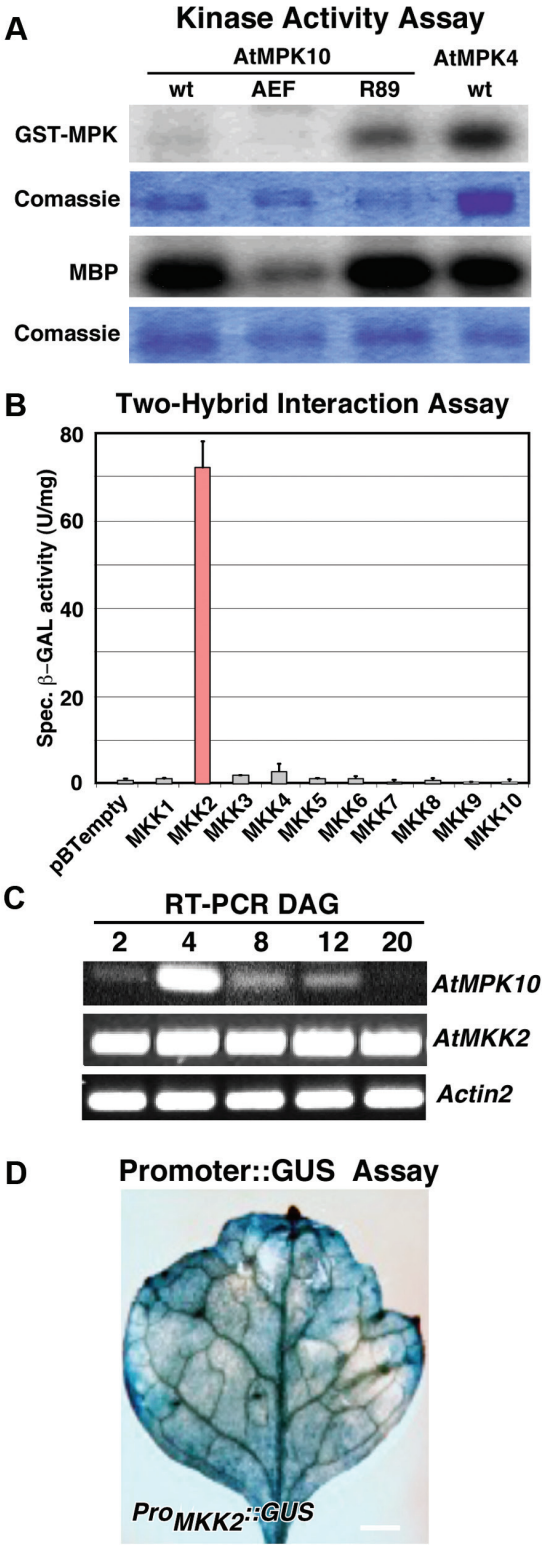

Figure 2 AtMPK10 Kinase Activity, Interaction, and Co-Expression with AtMPKK2.

(A) *In vitro* kinase assays of AtMPK10 wild-type (wt) and two mutant versions (AEF and R89) compared to AtMPK4 with myelin basic protein (MBP) as substrate. AtMPK10 wt has kinase activity similar to AtMPK4, whereas activity of the AEF mutant is reduced almost to background levels.

(B) Yeast two-hybrid interaction assays. AtMPK10 fused to the binding domain was tested for interaction with all known 10 *Arabidopsis* MKKs. According to enzymatic detection of β-GAL expression, a specific interaction exclusively occurred between AtMPK10 and AtMKK2. Columns indicate the average of specific β-GAL activity (n = 3). Bar = standard error of the means.

(C) RT–PCR revealed that the interacting proteins AtMPK10 and AtMKK2 are co-expressed in early developmental stages. AtMPK10 transcription is generally low, peaking at 4 days after germination whereas AtMKK2 transcription is relatively high during all stages.

(D) Histochemical localization of GUS activity of Pro_{AtMPK2}*::GUS* plants.

Figure 2C, expression of *MPK10* and *MKK2* overlapped in developing leaves, but only in a very narrow time window from 2 to 12 DAG with a strikingly sharp peak at 4 DAG. Moreover, expression analysis using an 801-bp-long promoter region of *MKK2* in a binary GUS reporter construct revealed also a partially overlapping expression pattern of *MPK10* and *MKK2* in leaves, with generally higher levels and a wider local distribution for *MKK2* (Figure 2D).

atmpk10 Plants Show a Delay in Shoot Outgrowth and Flowering

This extremely narrow time window of *MPK10* expression gave rise to the question for a visible phenotype. We found that *atmpk10* mutant lines did not show any germination or root elongation defects when compared to wild-type plants (Figure 3A). Furthermore, we tested various hormone and abiotic stress conditions to investigate a potential function of *MPK10* in development and stress responses. Mutant plants were exposed to the hormones abscisic acid (ABA) or indole-3-acetic acid (IAA), to the stress factors mannitol (osmotic stress), sodium chloride (salt stress), or salicylic acid (biotic stress), or were exposed to drought stress. As exemplified in Figure 3B for salicylic acid (SA), no obvious differences in germination rate or plant growth could be observed between *mpk10* and *Col-0* wild-type plants in any instance. Also at later stages, when plants were grown under short-day conditions (8-h light) for vegetative growth, no apparent differences with wild-type plants were seen (Figure 3C).

A different picture emerged when *atmpk10* plants were grown in long-day conditions (16-h light). *atmpk10* plants displayed a delay in flowering time of approximately 1 week as compared to wild-type plants. This effect became even more pronounced when *mpk10* plants were exposed to permanent light: they bolted at the same time as under long-day conditions while wild-type plants did so 1.5 weeks earlier (Figure 3D). Cotyledons of *atmpk10*

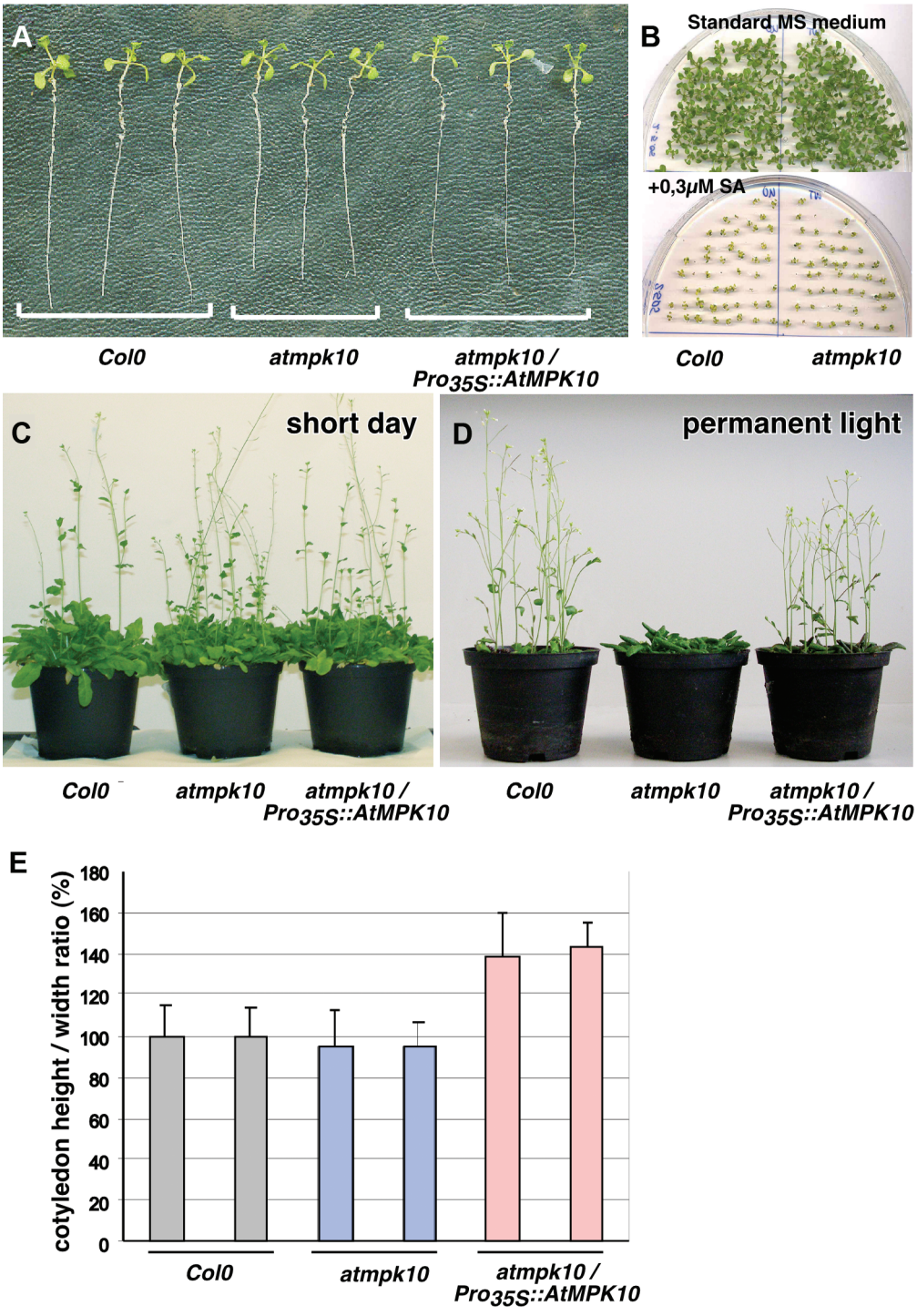

Figure 3 Phenotypical Analysis of *atmpk10* Mutants.

(A) Morphology: *atmpk10* and *atmpk10*/Pro_{35S}::*AtMPK10* seedlings show no obvious morphological differences compared to Col-0 wild-type plants.

(B) Germination rate and stress sensitivity: as exemplified with plants grown on MS-agar plates supplied with 0.3 μM salicylic acid (SA), *atmpk10* seedlings exposed to various stress conditions resemble wild-type plants in their growth and germination rate.

(C, D) Flowering time: (C) under short-day conditions, *atmpk10* plants are not delayed in flowering compared to (D) atmpk10 plants grown under permanent-light conditions. Note that the delay in flowering is restored in transgenic *atmpk10*/Pro_{35S}::*AtMPK10* lines overexpressing AtMPK10.

(E) Organ size: *AtMPK10* overexpression in the *atmpk10*/Pro_{35S}::*AtMPK10* produces seedlings with larger cotyledons compared to Col-0 wild-type and *atmpk10* mutant lines; $n > 30$; bar = standard deviation of the means.

plants were slightly smaller than in wild-type. Transgenic *atmpk10*/*Pro*$_{35S}$*::AtMPK10* plants formed larger cotyledons (Figure 3E). Together, these results implied that *mpk10* is a conditional mutant with respect to flowering. In addition, these data are in line with the notion that AtMPK10 is not involved in stress responses, but rather in the transition to flowering.

AtMPK10 and *AtMKK2* Assist in the Formation of Leaf Veins

The observed *AtMPK10* promoter activity in veins, the altered size of cotyledons, and the delayed flowering phenotype prompted us to study the potential role of the AtMKK2/AtMPK10 kinase cascade in vascular development. In cotyledons, the number of secondary vein loops originating from the midvein served as an indicator for vein complexity. As defined by Cnops et al. (2006), veins appearing on cotyledons can be classified into five groups representing increasing venation complexity (Figure 4A). The first group (simple closed) represents cotyledons showing the lowest complexity with two secondary loops. Group 2 (medium open) have three secondary vein loops and in group 3 (medium closed) they are connected with each other. Group 4 (complex open) represents patterns with two secondary vein loops plus one or two not fully connected veins. Cotyledons with four connected secondary loops originating from the midvein show a maximum of complexity and constitute group 5 (complex).

We inspected vein complexity in cotyledons of *Arabidopsis* wild-type, *mpk10*, and *mkk2* knockout lines (Teige et al., 2004), respectively. In Figure 4B, we present the percentage of cotyledons of wild-type (Col0), *mpk10*, and *mkk2* seedlings falling in one of the five venation complexity groups in relation to wild-type plants. In the mutants, the frequency of cotyledons with simple venation patterns (groups 1 and 2) was approximately 10% higher compared to the wild-type, while the frequency of those with higher complexity (groups 3 to 5) was decreased accordingly (Figure 4B). Both, *mpk10* and *mkk2* mutant lines had a significantly less complex venation architecture compared to wild-type. Cotyledon venation was even less complex (group 5) in *mpk10* than in *mkk2* mutants.

Complementation of the *atmpk10* Phenotype Depends on AtMPK10 Kinase Activity

In order to prove that the observed difference in cotyledon size, venation, and delay in bolting all resulted from a lack in AtMPK10 activity, we transformed the *atmpk10* mutant with a wild-type and a LOF allele of *AtMPK10*, both under control of the strong *CaMV35S* promoter, and confirmed their expression by RT–PCR and immunoprecipitation in

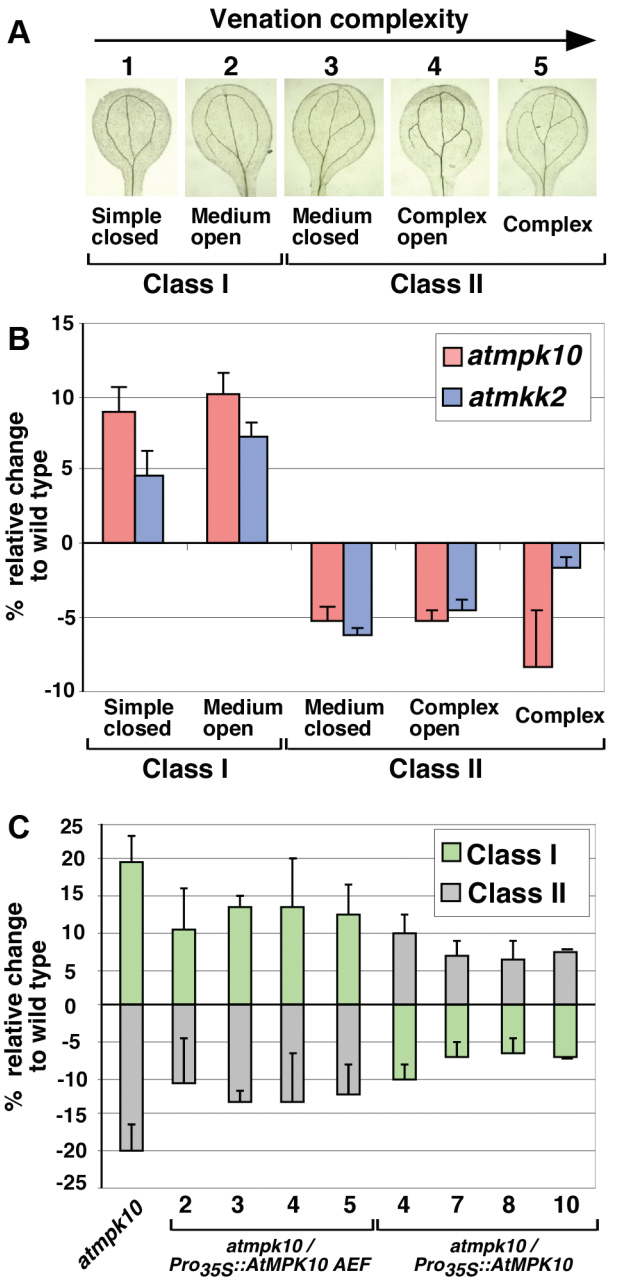

Figure 4 Venation Pattern of *atmpk10* and *atmkk2* Mutants.

(A) Grouping of venation patterns with increasing complexity (1 to 5) measured as number of proximal secondary vein loops originating from the midvein.

(B) Venation complexity of *atmpk10* and *atmkk2* mutants relative to wild-type Col-0 plants. Percentages of the total numbers of checked cotyledons (n > 150) are calculated as relative changes to Col-0 plants (baseline). Seedlings of both mutants show an increased number of cotyledons with patterns 1 and 2 (class I, low complexity) and a reduced number of patterns 3 to 5 (class II, high complexity).

(C) Graph presenting class I and class II cotyledons (n > 150) for transgenic atmpk10 mutant lines (n = 4) expressing the LOF

independent transgenic lines (Supplemental Figure 1). Expression of AtMPK10 in *atmpk10* plants resulted not only in a restoration of cotyledon size to wild-type levels, but to cotyledons that were significantly (40%) larger than wild-type (Figure 3E) while expression of the LOF allele did not restore size.

For simplicity and to emphasize the differences, we categorized the five venation pattern groups into two classes (Figure 4A). Groups 1 and 2 representing simple vein architecture were pooled in class I. Groups 3 to 5 representing high vein complexity were pooled in class II. While the frequency of simple venation patterns was approximately 20% higher in *atmpk10* lines than in wild-type, the transgenic *mpk10* lines expressing the LOF construct (*Pro$_{35S}$::AtMPK10 AEF*) showed an approximately 10%–15% lower complexity (Figure 4C). Moreover, expression of the wild-type allele under control of the strong CaMV-35S promoter (*Pro$_{35S}$::AtMPK10*) in *mpk10* plants shifted the venation pattern in the opposite direction, thus confirming that AtMPK10 kinase activity is required for establishing a complex venation architecture. Notably, the rate of more complex venation patterns in these lines increased up to 10% over wild-type levels.

Finally, the flowering time phenotype of the *mpk10* mutant was also restored by overexpression of AtMPK10 in an *atmpk10* background. As with leaf size and vein patterning, a gain-of-function phenotype could be observed in that *Pro$_{35S}$::AtMPK10* plants in an *atmpk10* background flowered at a time similar to wild-type plants. Because these transgenic lines did not contain a functional endogenous *AtMPK10* gene, the gain-of-function phenotype must have been caused by complementation and not by an accidental activation of the endogenous gene as may happen in overexpressing lines in a wild-type background (Weigel et al., 2000).

AtMPK10 Expression Coincides with Sites of Auxin Maxima but Is Not Affected by Auxin

An important observation was that *AtMPK10* expression in leaf regions coincided with auxin production or accumulation sites observed with the auxin-responsive element *DR5* (Benkova et al., 2003; Friml et al., 2003). This suggested that *AtMPK10* expression might be regulated by auxin and/or that AtMPK10 kinase activity could regulate auxin levels (i.e. production or transport). Stipules are the earliest sites of auxin production during leaf development, followed by a shift to the elongating leaf tip to induce the primary vein and then to the hydathodes to induce secondary veins. At a later stage, auxin is produced in the leaf lamina by mesophyll cells and trichomes, inducing the tertiary and quaternary veins.

First, we tested whether the *AtMPK10* promoter activity was controlled by auxin. *Pro$_{AtMPK10}$::GUS* plants grown on MS medium were treated with increasing concentrations of indole acetic acid (IAA) and *AtMPK10* expression was followed by GUS staining (Figure 5A–5D). For this purpose, plants were either grown on MS medium containing 1 μM IAA (Figure 5A) or were infiltrated 7 DAG with 10 μM or 100 μM IAA and tested for GUS activity 1 d later (Figure 5C). In all instances, no evident changes in AtMPK10 promoter-driven GUS activity were observed (Figure 5A–5D), which was confirmed by semi-quantitative RT–PCR on wild-type plants (data not shown). These observations implied that *AtMPK10* expression is not regulated by auxin. Also, infiltration of *mpk10* mutant leaves with low amounts of auxin (1 μM) had no effect on vein patterning.

Next, to uncover a link between *AtMPK10* expression and PAT, we exposed *Pro$_{AtMPK10}$::GUS* plants to different concentrations of the PAT inhibitor HFCA. To visualize the effect of PAT inhibition, we used the well-characterized auxin reporter line *Pro$_{DR5}$::GFP* (Benkova et al., 2003; Friml et al., 2003) and compared the GFP signal (indicating auxin concentrations) to *AtMPK10* promoter-driven GUS expression (Figure 5E–5J). In control *Pro$_{AtMPK10}$::GUS* plants, GUS activity was highest in cotyledons at the distal margin of the midvein (Figure 5B) and at the hydathodes in fully expanded rosette leaves (Figure 5D). Presence of low amounts of HFCA (5 μM) resulted in an increased *Pro$_{AtMPK10}$::GUS* activity at the midvein and the tip (Figure 5E) that did not coincide with an increased expression of the *Pro$_{DR5}$::GFP* auxin sensing lines (Figure 5F). Rather, *Pro$_{DR5}$::GFP* plants showed an increased GFP signal at the leaf margins and veins (Figure 5F). Treatment of both transgenic reporter lines with higher amounts of HFCA (40 μM and 100 μM) caused higher GUS and GFP activity in cotyledons and thicker, misshaped veins, a reduction in cotyledon size, and an elongation of rosette leaves (Figure 5G–5J). In general, *Pro$_{AtMPK10}$::GUS* activity coincided with the GFP signal from the auxin reporter line at the leaf tip, the leaf margins, and vasculature (Figure 5F, 5H, and 5J, and Supplemenal Figure 2), similarly to that described for auxin distribution (Mattsson et al., 1999; Sieburth, 1999; Mattsson et al., 2003). Thus, inhibition of auxin transport increased the area of auxin maxima sites in the leaf concomitantly with an increase in *AtMPK10* expression.

The increase of *AtMPK10* transcriptional activity in wild-type seedlings exposed to HFCA was confirmed by RT–PCR. A higher but transient AtMPK*10* signal was detected at 4 and 8 DAG after exposure to 5 μM and 40 μM HFCA (Figure 5K) relative to untreated seedlings (Figure 2B) that disappeared at 12 DAG. *AtMPK10* expression showed an

AtMPK10 AEF construct devoid of kinase activity (*atmpk10/Pro$_{35S}$::AtMPK10 AEF*) or overexpressing *AtMPK10* cDNA (*atmpk10/Pro$_{35S}$::AtMPK10*). Values are presented in percentage of relative changes to the Col-0 wild-type (baseline).

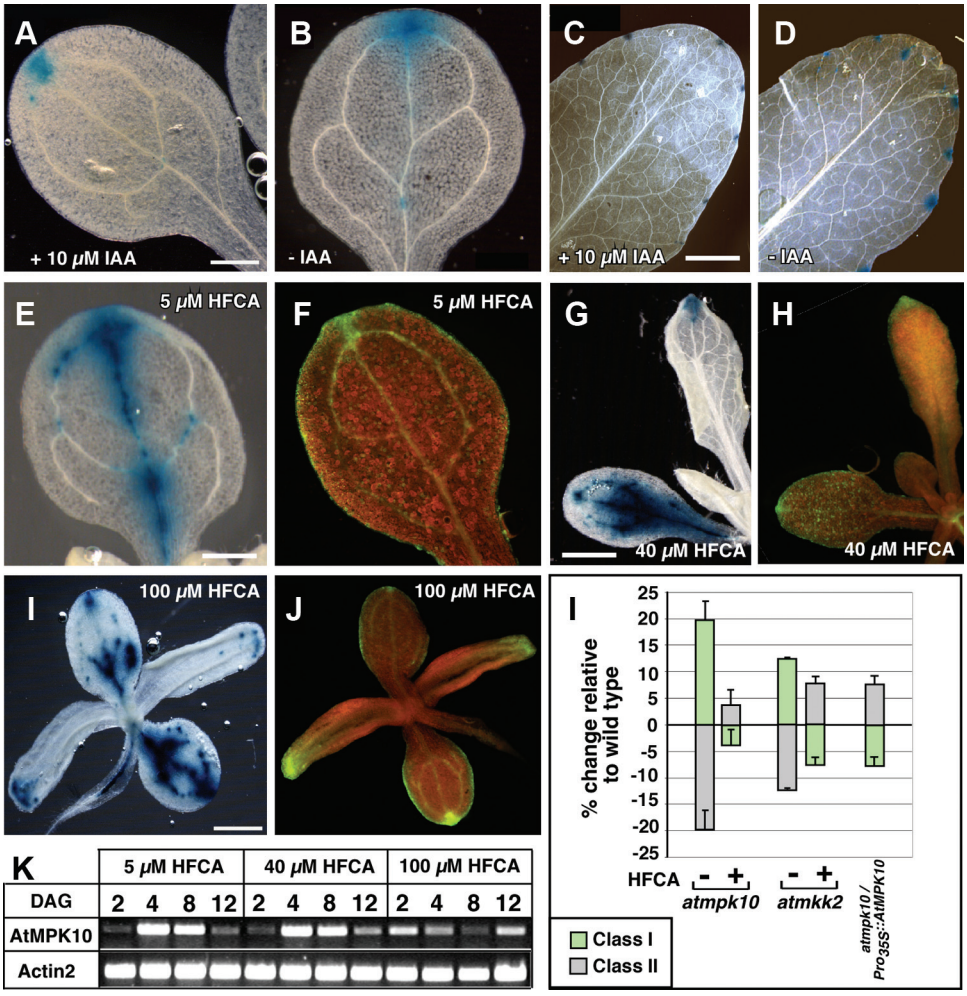

Figure 5 Effect of Auxin and Auxin Transport Inhibition on *AtMPK10* Promoter Activity and Vascular Development of *atmkk2* and *atmpk10* Plants.

(A–D) IAA treatment of $Pro_{AtMPK10}$*::GUS* reporter lines visualized by GUS signals in the presence of 10 μM IAA 12 days after germination (DAG) (A, B) or 28 DAG (C, D).

(E–J) Independent $Pro_{AtMPK10}$*::GUS* and Pro_{DR5}*::GFP* reporter lines treated with the PAT inhibitor HFCA and imaged in parallel via a binocular microscope at the same growth stage. (E) GUS activity in the midvein and the tip of cotyledons in the presence of 5 μM HFCA. (F) Pro_{DR5}*::GFP* expression in the tip and marginal regions of the cotyledons. (G) *AtMPK10* promoter activity in seedlings grown on 40 μM HFCA and (H) auxin accumulation in the vasculature of cotyledons and the leaf-tip. (I, J) Seedlings grown on 100 μM HFCA lose their natural shape. (I) High promoter activity (GUS) and (J) auxin accumulation (GFP) at the leaf tips and margins.

(K) RT–PCR analysis of *AtMPK10* expression in response to HCFA (compare to Figure 1K).

(L) Changes in venation complexity of *atmpk10* and *atmkk2* seedlings grown on MS medium without (–) or with 5 μM HFCA (+). As indicated in Figure 4, venation patterns of cotyledons were classified into class I (low complexity) and class II (high complexity). Values are given in percentages of relative changes to untreated Col-0 wild-type seedlings (baseline). Note that the mutant venation phenotype reversed and is very similar to untreated atmpk10 overexpressor seedlings (*atmpk10*/Pro_{35S}*::AtMPK10*) shown as a control (right column).

increase at all time points tested upon treatment with 100 μM HFCA, congruent with the higher GUS signal in $Pro_{AtMPK10}$*::GUS* plants. In summary, the observed changes of *AtMPK10* expression in response to inhibition of auxin transport implied a functional connection between *AtMPK10* and PAT in *Arabidopsis*.

AtMKK2 and *AtMPK10* Modulate Auxin Transport

Since it is well known that inhibition of PAT has an effect on vessel formation in cotyledons and since we had found that *AtMPK10* expression was affected by auxin

transport inhibition but not by exogenous auxin, we tested whether PAT inhibition affects vein patterning in the *atmpk10* mutant. Exposing cotyledons of mutants lacking *AtMPK10* or *AtMKK2* activity to HFCA treatment (5 μM) restored the venation pattern to wild-type levels (Figure 5L). The fact that the PAT inhibitor HFCA was able to restore the mutant vein pattern similarly to molecular complementation by *AtMPK10* suggested that a block of auxin efflux may be required for normal vascular development and that AtMPK10 may be involved in auxin allocation.

DISCUSSION

MAPKs are involved in a wide array of cell signaling pathways, and there is evidence that they are key regulators of developmental decisions and of biotic and abiotic stress responses (Bergmann and Sack, 2007; Rodriguez et al., 2010). Here we show that plants lacking AtMPK10 or AtMKK2 activity have smaller leaves and a less complex vein pattern. Plants devoid of MPK10 also show delayed bolting and flowering under long-day conditions. A very similar phenotype has been described for AtMKK7 overexpressing lines that were suggested to have an impaired PAT system (Dai et al., 2006). Similarly, inhibiting polar auxin transport (PAT) was able to restore the venation phenotype to wild-type in *mpk10* and *mkk2* mutants. The *atmpk10* phenotype could be restored by overexpression of AtMPK10 exhibiting kinase activity, but not by a LOF AtMPK10 construct. The complemented mutant showed a gain-of-function phenotype with larger cotyledons and a more complex vein pattern than wild-type plants indicating that both AtMPK10 and AtMKK2 may act antagonistically to MKK7. This supports the notion that AtMPK10 activity is necessary for and has a regulatory role in auxin transport, vascular formation, leaf growth, and the transition to flowering in long days.

MKK2/MPK10 Function in Venation

AtMPK10 promoter activity studies revealed a specific expression pattern overlapping with areas of auxin maxima (production or accumulation) at restricted vein areas, leaf tips, and serrated leaf margins representing hydathodes. This is in contrast to the other two group A MAPKs *AtMPK3* and *AtMPK6*, which have dual functions in stomatal development and patterning, and stress responses, respectively. *AtMPK3* and *AtMPK6* are both induced strongly upon exposure to biotic and abiotic stresses. Under normal conditions, *AtMPK3* is highly expressed in leaves and roots, and *AtMPK6* is ubiquitously expressed (Bush and Krysan, 2007). Notably, *mpk3/mpk6* double mutants are embryo-lethal, thus indicating that these two MAPKs are also involved in important developmental processes other than stomata development (Hord et al., 2008). In line with a low expression recorded in microarray experiments (Winter et al., 2007), we observe a very transient and highly restricted expression pattern of *AtMPK10* (Figures 1 and 5, and Supplemental Figure 3). *AtMPK10* has also been annotated as a seed-specific gene in a comprehensive study using Laser-Capture Microdissection (LCM) to obtain a high spatial and temporal resolution of mRNA profiles during seed development (Belmonte et al., 2013). *MKK2* expression has been detected during all stages of seed development in that study. In our view, this annotation is also due to the narrow time window of *AtMPK10* expression in the very early steps of leaf development. For functional studies, this is a key observation, because many large-scale proteomics and interactomis studies cannot consider the endogenous expression levels per se, and many phenotypes reported so far result from ectopic overexpression. Accordingly, it is not surprising that the developmental phenotype we describe here for the *mpk10* mutant has not been observed in previous studies because a stress-related phenotype had been expected based on the function of the two other group A MAPKs. In our yeast two-hybrid interaction assays, we found AtMKK2 as upstream kinase of AtMPK10, which is consistent with previous reports on protein interaction (Lee et al., 2008; Andreasson and Ellis, 2010) and *in vitro* phosphorylation data (Popescu et al., 2009). *AtMKK2* and *AtMPK10* showed spatially and temporally overlapping expression patterns in our studies as well as in published data sets and available online resources such as the Arabidopsis eFP Browser (Winter et al., 2007). Thus, AtMKK2 seems to operate also in an additional signaling pathway unrelated to stress, which is active only during a very narrow time window during plant development.

A delayed flowering phenotype was observed with *mpk10* plants exposed to long-day or permanent-light conditions. These plants had smaller cotyledons and showed also reduced vein pattern complexity. All three phenotypes could be restored by a functional *AtMPK10* construct transformed into *mpk10* mutant plants but not by a LOF version lacking kinase activity indicating that AtMPK10 kinase activity is required for normal plant development. A similar loss of venation complexity was observed in *mkk2* mutants; their venation patterns were nearly identical to *atmpk10* plants. Together with the overlapping expression patterns, this supports a functional interaction of AtMPK10 and AtMKK2 in the regulation of vein formation during leaf development. The gain-of-function phenotype in *atmpk10* plants transformed with *AtMPK10* expressed by a strong promoter indicates further that AtMPK10 is also involved in the transition to flowering.

Mutants in genes such as *AUXIN-RESISTANT 1* (Lincoln et al., 1990), *MONOPTEROS* (Wenzel et al., 2007), *SCARFACE* (Deyholos et al., 2000), *BODENLOS* (Hamann et al., 1999, 2002), *FORKED* (Steynen and Schultz, 2003),

PIN FORMED 1 (*PIN1*) (Galweiler et al., 1998), and *PINOID* (Christensen et al., 2000) all have overlapping phenotypes with *atmpk10* and overlapping relationships to auxin and auxin transport. For example, mutations in the kinase *PINOID* (*PID*), encoding a component of the efflux carrier system, shows increased vascularization close to the leaf margins (Mattsson et al., 1999; Steinmann et al., 1999) while *scarface* mutants show, like *atmpk10*, reduced vein complexity and delayed flowering (Deyholos et al., 2000). It remains to be seen how *AtMKK2* and *AtMPK10* interact with these genes.

Interestingly, Dai et al. (2006) described a MAPK mutant with a phenotype quite similar to *mpk10* and *mkk2* that was also related to PAT. They reported a reduced vein complexity phenotype in plants overexpressing AtMKK7. In contrast, overexpression of AtMKK2 and AtMPK10 resulted in a more complex vein pattern while a reduced vein pattern was seen in mutants lacking AtMKK2 or AtMPK10 function. Thus, two different MAPK signaling modules seem to be involved in PAT and vessel formation; one (i.e. the AtMKK2/AtMPK10 module) positively regulating PAT, leaf size, and vessel formation, and another (i.e. the AtMKK7 module) as negative regulator of these processes. However, an unexpected positive regulatory role in leaf development for AtMKK7 and AtMKK9 has also recently been reported (Lampard et al., 2009).

Leaves are able to adapt to changing environmental conditions. Nutrients and florigenic signals, which are produced in leaves, are relayed via the phloem to the shoot apex (Corbesier et al., 2007; Lin et al., 2007). The effect on flowering time was seen only in *mpk10* mutant plants grown under long-day conditions, which promote flowering of *Arabidopsis*. The AtMKK2/AtMPK10 module seems therefore to be part of a pathway involved in photoperiod-sensing but not in the autonomous vernalization or gibberellin signaling of flower induction. Alternatively, it may be that the delay of flowering in the *mpk10* mutant is a passive consequence of inefficient transport of nutrients and florigenic signals by altered vessel numbers. RT–PCR indeed detected *AtMPK10* transcripts in stem and root, and GUS staining was observed in embryos of *AtMPK10*-promoter::GUS plants indicating that AtMPK10 may be involved in vessel formation throughout the plant body.

The MKK2/MPK10 MAP Kinase Cascade Regulates Venation by Modulating Auxin Signaling

AtMPK10 expression at leaf margins resembled, at least partially, that of the auxin sensitive *DR5*-promoter line in the leaf tip, the hydathodes, and other sites in the leaves. Thus, we asked whether AtMPK10 expression is regulated by auxin. This could be ruled out, as exogenously applied auxin had no effect on AtMPK10 transcriptional activity. Another possibility was that AtMPK10 would be involved in the regulation of PAT. Indeed, treatment of *atmpk10* mutants with the PAT inhibitor HFCA resulted in the rescue of vein pattern complexity in leaves of *mpkk2* and *mpk10* plants to wild-type levels. In contrast, auxin treatment of *AtMPK10* promoter reporter lines did not result in a detectable increase in AtMPK*10* transcriptional activity.

These results pointed to a possible role of the AtMKK2/AtMPK10 kinase cascade in PAT controlling vascular development (Figure 6). As treatment of the *mpk10* mutant with PAT inhibitors had the same effect as expression of AtMPK10 or AtMKK2 in this mutant background, it seems that the AtMKK2/AtMPK10 module plays a role in the action of PAT inhibitors. PAT inhibitors such as HFCA, NPA, or TIBA are synthetic substances but it is widely accepted that they mimic the action of natural PAT inhibitors (Murphy et al., 2000).

The *atmpk10* and *atmkk2* phenotypes, *AtMPK10* and *DR5* expression patterns, the effect of *AtMPK10*/*AtMKK2* overexpression, and of HFCA treatment can be incorporated into a model that is based on and extends the auxin canalization model of Sachs (1991) or 'leaf-margin guided' venation model (Scheres and Xu, 2006) and the 'auxin efflux transporter convergence point' venation model by Scarpella et al. (2006). In such a model (Figure 6), based on the observed HFCA-mediated rescue of the mutants, the AtMKK2/AtMPK10 signaling module seems to negatively regulate PAT at sites of the leaf margins at which auxin maxima are being created. These sites may have been produced by convergent auxin transport via efflux carriers (Scarpella et al., 2006) or by auxin synthesis at these sites. PAT inhibitors block auxin efflux carriers such as PINs or PGPs in these cells and prevent export of auxin from these sites, in effect being required—together with auxin transport to or auxin synthesis at these sites—for the creation of local auxin maxima that serve as starting sites for vessel formation. Here AtMKK2/AtMPK10 could control the number and 'strength' of auxin maxima and thus the number and length of vascular strands, namely vein patterning. The fact that PAT inhibitors provoke more auxin convergence points (Scarpella et al., 2006) is fully compatible with this model and our observation that HFCA treatment reverses the vein pattern phenotype of *atmpk10* mutants. Last but not least, the recent analysis of different mutants affected in leaf venation patterns does further underpin the functional link between leaf venation and PAT (Tsugeki et al., 2009; Hou et al., 2010; Robles et al., 2010). The identification of a number of auxin-related transcription factors as potential MAP kinase targets (Popescu et al., 2009) together with the proposed link to inositol metabolism and *trans*-Golgi trafficking (Hou et al., 2010) points further towards a complex regulatory network of leaf venation providing a lot of space for future investigations.

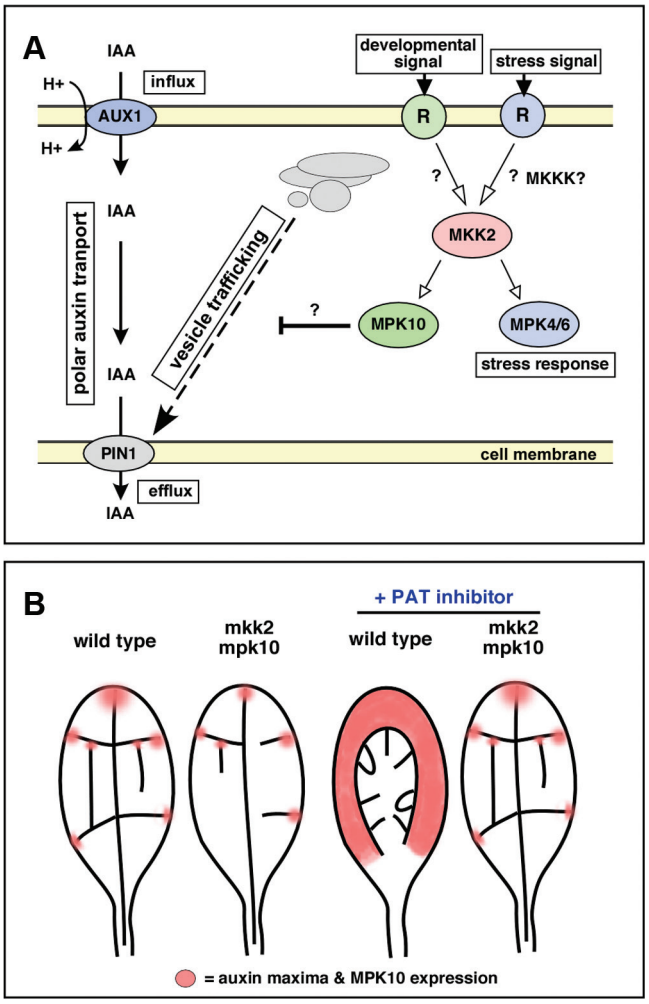

Figure 6 Putative Model for the Function of the AtMKK2/AtMPK10 Kinase Cascade on PAT and Vascular Development.

(A) MKK2 and MPK10 affect directly or indirectly the vesicle trafficking efficiency within the vascular precursor cells. This affects also the transport of the auxin carrier to the cell membrane thereby altering the polar auxin transport and vascular development (for detailed explanation, see the 'Discussion' section).

(B) The effect of MKK2/MPK10 on leaf vascular development in the context of auxin channeling. The model integrates known effects of PAT inhibitors on wild-type leaves, *AtMPK10* and *DR5* expression patterns (= auxin maxima), *atmpk10* and *atmkk2* mutant phenotypes, AtMPK10 overexpression, and treatment of the mutants with the PAT inhibitor HFCA. Here the MKK2/MPK10 kinase cascade controls number and 'strength' of auxin maxima (red) as starting sites for provascular strands formation. In *mpk10* and *mkk2* mutant plants, auxin maxima are fewer and in smaller areas leading to a less complex vasculature. Thus, plants lacking MPK10 or MKK2 activity are less sensitive to PAT inhibitors and form a vasculature exhibiting a similar complexity to the wild-type.

METHODS

Plant Growth

Arabidopsis thaliana seeds were stratified for 2 d at 4°C and germinated either in a mixture of 3:1 soil/sand or in MS plant medium with 0.5 g L^{-1} sucrose (Sigma). All plants were grown at 21°C and a medium light intensity of 200 µE (cool white light) under long-day conditions (16-h light) or under permanent-light conditions in a controlled environment chamber (Percival). NaCl, SA, mannitol, abscisic acid, IAA, and HFCA solutions were autoclaved or filter sterilized and added to MS medium before seed germination.

Analysis of the *mpk10* T-DNA Insertion Mutant and Cloning of AtMPK10

For the primer sequences used, see Supplementary Data. The *atmpk10* mutant was obtained from the SALK T-DNA mutant collection (http://signal.salk.edu/cgi-bin/tdnaexpress, Stock number N539102). Genomic DNA submitted to PCR analysis was extracted as described (Edwards et al., 1991). DNA for Southern analysis was extracted with a DNeasy Plant Kit (Qiagen). Homozygous T-DNA insertion lines were verified by PCR using AtMPK10 (At3g59790) specific primers 5′ AtMPK10KO, 3′ primer AtMPK10.1501, and 5′-T-DNA LB-SALK primer, and by sequencing the PCR fragments. Southern blot analysis was performed with genomic DNA (10 µg) digested with *Nco*I and *Nde*I/*Hin*dIII. A non-radioactive labeling system (Gene Images Random Prime Labelling Module; Amersham) was used according to the manufacturer's instructions to detect specific DNA fragments. RT–PCR analysis was carried out with total RNA prepared with the RNeasy Mini Kit (Qiagen) and treated with DNase I (Roche) prior to RT–PCR reaction (Thermo-Script™ RT–PCR system, Invitrogen). For the RT reaction a poly-T primer and for PCR amplification the following primer pairs were used for AtMKK2 (At4g29810): AtMKK2.5′ and AtMKK2.3′; for AtACTIN2 (At3g18780): AtACTIN2-5′ and AtACTIN2-3′. For AtMPK10 cDNA and promoter cloning and mutagenesis procedures, see Supplementary Data.

Protein Extraction, Western-Blot, and Immune-Precipitation

Proteins were extracted from approximately 150 mg of *Arabidopsis* leaves in 200 µl of Locus Buffer as described in Bogre et al. (1999). The suspension was mixed thoroughly and centrifuged (15 000 rpm; 15 min) at 4°C. The supernatant (50 µg protein) was submitted to SDS–PAGE as described (Wilson et al., 1997) and transferred onto nitrocellulose membranes (Amersham). After blocking with 5% fat-free dry milk, the membrane was incubated overnight with 1:5000 diluted primary HA antibody (mono-HA,

Covagene) followed by detection with secondary ALP-conjugated antibody (Sigma). Immunoprecipitation was performed as described (Limmongkon et al., 2004) with the following modifications. An additional pre-clearing step of the crude protein lysate with 50 µl of 50% slurry of protein A sepharose beads (Amersham) was carried out for 1 h at 4°C. The supernatant was then immuno-precipitated using the HA antibody (mono-HA, Covanance).

Expression and Purification of GST-Fusion Proteins and *In Vitro* Kinase Assays

AtMPK10 cDNA (wild-type and mutant versions) were cloned as *Nco*I/*Not*I fragments into pGEX4T1 (Amersham) and expressed as C-terminal glutathione S-transferase (GST) fusion proteins. GST purification was carried out using glutathione sepharose TM4B (Amersham) according to the manufacturer's instructions. AtMPK10–GST protein fractions were eluted with the reduced glutathione buffer solution (33 mM reduced glutathione, 250 mM NaCl, 0.5% Triton-X100 in 1 TBS), which was replaced by 1 kinase buffer (20 mM HEPES pH 7.5, 15 mM $MgCl_2$, 8 mM EDTA, 1 mM DTT) using PD10 columns (Amersham) to allow *in vitro* protein kinase assays with MBP as generic substrate as described (Teige et al., 2004).

GUS Reporter Assays and Venation Pattern Analysis

The promoter regions (700 bp for *AtMPK10* and 801 bp for *AtMKK2*, respectively) were amplified by PCR from genomic DNA and cloned into the binary pGreenII 0029 GUS vector (Hellens et al., 2000) for the generation of stable plant reporter lines by floral dipping (Clough and Bent, 1998). Plant organs were vacuum-infiltrated for 1 min with a staining solution containing 1 mM 5-bromo-4-chloro-3-indoyl-D-glucuronide (X-Gluc; JERSY LAB SUPPLY) at pH 7, 0.1% Triton 10 mM EDTA, 0.5 mM potassium ferrocyanide, and 0.5 mM potassium ferricyanide, followed by an incubation at 37°C for 12–24 h. Samples were de-stained in 1:1 clearing solution of ethanol and acetic acid for 24 h and analyzed with a stereomicroscope equipped with an integrated digital camera (Leica MZ16FA, Zeiss STEMI 2000-C).

Microscopy

The images were obtained with a Leica Stereomicroscope (MZ12) equipped with a Leica color detection camera (DFC300FX), Leica Application Suit (LAS) software, equipped with a fluorescence light source and standard GFP long-pass filter system allowing the simultaneous detection of GFP (appearing green) and plastid auto-fluorescence (appearing red). The exposure time was set at <15 s to avoid unspecific green auto-fluorescence.

Two-Hybrid Interaction Assays

Quantitative yeast two-hybrid assays were performed as described (Teige et al., 2004) using the yeast strain L40 and the vectors LexA–BD pBTM116 (Vojtek, 1993) for the BD–MKK fusions and pGAD424 (Clontech, USA) for the Gal4-AD fusion of AtMPK10. All constructs were cloned as *Nco*I/*Not*I fragments into the pBTM116 vector or into the pGAD vector as described in Teige et al. (2004).

SUPPLEMENTARY DATA

Supplementary Data are available at *Molecular Plant Online*.

FUNDING

This work has been supported by the Austrian Science Fund (FWF) with projects P16640 to E.H.B., project P19682 to F.K., and P24335 to M.T., respectively.

ACKNOWLEDGMENTS

The authors thank Christine Abel and Aleksandra Pietrzyk for technical support. No conflict of interest declared.

REFERENCES

Andreasson, E., and Ellis, B. (2010). Convergence and specificity in the *Arabidopsis* MAPK nexus. Trends Plant Sci. **15**, 106–113.

Asai, T., Tena, G., Plotnikova, J., Willmann, M.R., Chiu, W.L., Gomez-Gomez, L., Boller, T., Ausubel, F.M., and Sheen, J. (2002). MAP kinase signalling cascade in *Arabidopsis* innate immunity. Nature. **415**, 977–983.

Avsian-Kretchmer, O., Cheng, J.C., Chen, L., Moctezuma, E., and Sung, Z.R. (2002). Indole acetic acid distribution coincides with vascular differentiation pattern during *Arabidopsis* leaf ontogeny. Plant Physiol. **130**, 199–209.

Belmonte, M.F., Kirkbride, R.C., Stone, S.L., Pelletier, J.M., Bui, A.Q., Yeung, E.C., Hashimoto, M., Fei, J., Harada, C.M., Munoz, M.D., et al. (2013). Comprehensive developmental profiles of gene activity in regions and subregions of the *Arabidopsis* seed. PNAS. **110**, E435–E444.

Benkova, E., Michniewicz, M., Sauer, M., Teichmann, T., Seifertova, D., Jurgens, G., and Friml, J. (2003). Local, efflux-dependent auxin gradients as a common module for plant organ formation. Cell. **115**, 591–602.

Bergmann, D.C., and Sack, F.D. (2007). Stomatal development. Annu. Rev. Plant Biol. **58**, 163–181.

Bergmann, D.C., Lukowitz, W., and Somerville, C.R. (2004). Stomatal development and pattern controlled by a MAPKK kinase. Science. **304**, 1494–1497.

Bernasconi, P. (1996). Effect of synthetic and natural protein tyrosine kinase inhibitors on auxin efflux in zucchini (*Cucurbita pepo*) hypocotyls. Physiologia Plantarum. **96**, 205–210.

Bogre, L., Calderini, O., Binarova, P., Mattauch, M., Till, S., Kiegerl, S., Jonak, C., Pollaschek, C., Barker, P., Huskisson, N.S., et al. (1999). A MAP kinase is activated late in plant mitosis and becomes localized to the plane of cell division. Plant Cell. **11**, 101–113.

Bush, S.M., and Krysan, P.J. (2007). Mutational evidence that the *Arabidopsis* MAP kinase MPK6 is involved in anther, inflorescence, and embryo development. J. Exp. Bot. **58**, 2181–2191.

Candela, H., Martınez-Laborda, A., and Micol, J.L. (1999). Venation pattern formation in *Arabidopsis thaliana* vegetative leaves. *Dev Biol*. **205**, 205–216.

Cardinale, F., Meskiene, I., Ouaked, F., and Hirt, H. (2002). Convergence and divergence of stress-induced mitogen-activated protein kinase signaling pathways at the level of two distinct mitogen-activated protein kinase kinases. Plant Cell. **14**, 703–711.

Christensen, S.K., Dagenais, N., Chory, J., and Weigel, D. (2000). Regulation of auxin response by the protein kinase PINOID. Cell. **100**, 469–478.

Clough, S.J., and Bent, A.F. (1998). Floral dip: A simplified method for grobacterium-mediated transformation of *Arabidopsis thaliana. Plant J*. 16, 735–743.

Cnops, G., Neyt, P., Raes, J., Petrarulo, M., Nelissen, H., Malenica, N., Luschnig, C., Tietz, O., Ditengou, F., Palme, K., et al. (2006). The TORNADO1 and TORNADO2 genes function in several patterning processes during early leaf development in *Arabidopsis thaliana*. Plant Cell. **18**, 852–866.

Colcombet, J., and Hirt, H. (2008). *Arabidopsis* MAPKs: a complex signalling network involved in multiple biological processes. Biochemical J. **413**, 217–226.

Corbesier, L., Vincent, C., Jang, S., Fornara, F., Fan, Q., Searle, I., Giakountis, A., Farrona, S., Gissot, L., Turnbull, C., et al. (2007). FT protein movement contributes to long-distance signaling in floral induction of *Arabidopsis.* Science. **316**, 1030–1033.

Dai, Y., Wang, H., Li, B., Huang, J., Liu, X., Zhou, Y., Mou, Z., and Li, J. (2006). Increased expression of MAP KINASE KINASE7 causes deficiency in polar auxin transport and leads to plant architectural abnormality in *Arabidopsis*. Plant Cell. **18**, 308–320.

Delbarre, A., Muller, P., and Guern, J. (1998). Short-lived and phosphorylated proteins contribute to carrier-mediated efflux, but not to influx, of auxin in suspension-cultured tobacco cells. Plant Physiol. **116**, 833–844.

Deyholos, M.K., Cordner, G., Beebe, D., and Sieburth, L.E. (2000). The SCARFACE gene is required for cotyledon and leaf vein patterning. Development. **127**, 3205–3213.

Duerr, B., Gawienowski, M., Ropp, T., and Jacobs, T. (1993). MsERK1: a mitogen-activated protein kinase from a flowering plant. Plant Cell. **5**, 87–96.

Edwards, K., Johnstone, C., and Thompson, C. (1991). A simple and rapid method for the preparation of plant genomic DNA for PCR analysis. Nucleic Acids Res. **19**, 1349.

Feilner, T., Hultschig, C., Lee, J., Meyer, S., Immink, R.G., Koenig, A., Possling, A., Seitz, H., Beveridge, A., Scheel, D., et al. (2005). High throughput identification of potential *Arabidopsis* mitogen-activated protein kinases substrates. Mol. Cell Proteomics. **4**, 1558–1568.

Friml, J., Vieten, A., Sauer, M., Weijers, D., Schwarz, H., Hamann, T., Offringa, R., and Jurgens, G. (2003). Efflux-dependent auxin gradients establish the apical–basal axis of *Arabidopsis*. Nature. **426**, 147–153.

Galweiler, L., Guan, C., Muller, A., Wisman, E., Mendgen, K., Yephremov, A., and Palme, K. (1998). Regulation of polar auxin transport by AtPIN1 in *Arabidopsis* vascular tissue. Science. **282**, 2226–2230.

Gray, J.E., and Hetherington, A.M. (2004). Plant development: YODA the stomatal switch. Curr. Biol. **14**, R488–R490.

Group, M. (2002). Mitogen-activated protein kinase cascades in plants: a new nomenclature. Trends Plant Sci. **7**, 301–308.

Hadfi, K., Speth, V., and Neuhaus, G. (1998). Auxin-induced developmental patterns in *Brassica juncea* embryos. Development. **125**, 879–887.

Hamann, T., Benkova, E., Baurle, I., Kientz, M., and Jurgens, G. (2002). The *Arabidopsis* BODENLOS gene encodes an auxin response protein inhibiting MONOPTEROS-mediated embryo patterning. Genes Dev. **16**, 1610–1615.

Hamann, T., Mayer, U., and Jurgens, G. (1999). The auxin-insensitive bodenlos mutation affects primary root formation and apical–basal patterning in the *Arabidopsis* embryo. Development. **126**, 1387–1395.

Hamel, L.P., Nicole, M.C., Sritubtim, S., Morency, M.J., Ellis, M., Ehlting, J., Beaudoin, N., Barbazuk, B., Klessig, D., Lee, J., et al. (2006). Ancient signals: comparative genomics of plant MAPK and MAPKK gene families. Trends Plant Sci. **11**, 192–198.

Hellens, R.P., Edwards, E.A., Leyland, N.R., Bean, S., and Mullineaux, P.M. (2000). pGreen: a versatile and flexible binary Ti vector for Agrobacterium-mediated plant transformation. Plant Mol. Biol. **42**, 819–832.

Hord, C.L., Sun, Y.J., Pillitteri, L.J., Torii, K.U., Wang, H., Zhang, S., and Ma, H. (2008). Regulation of *Arabidopsis* early anther development by the mitogen-activated protein kinases, MPK3 and MPK6, and the ERECTA and related receptor-like kinases. Mol. Plant. **1**, 645–658.

Hou, H., Erickson, J., Meservy, J., and Schultz, E.A. (2010). FORKED1 encodes a PH domain protein that is required for PIN1 localization in developing leaf veins. Plant J. **63**, 960–973.

Ichimura, K., Mizoguchi, T., Yoshida, R., Yuasa, T., and Shinozaki, K. (2000). Various abiotic stresses rapidly activate *Arabidopsis* MAP kinases ATMPK4 and ATMPK6. Plant J. **24**, 655–665.

Jensen, P.J., Hangarter, R.P., and Estelle, M. (1998). Auxin transport is required for hypocotyl elongation in light-grown but not dark-grown *Arabidopsis*. Plant Physiol. **116**, 455–462.

Jonak, C., Pay, A., Bogre, L., Hirt, H., and Heberle-Bors, E. (1993). The plant homologue of MAP kinase is expressed in a cell cycle-dependent and organ-specific manner. Plant J. **3**, 611–617.

Kerk, N.M., Jiang, K., and Feldman, L.J. (2000). Auxin metabolism in the root apical meristem. Plant Physiol. **122**, 925–932.

Khan, M., Rozhon, W., Bigeard, J., Pflieger, D., Husar, S., Pitzschke, A., Teige, M., Jonak, C., Hirt, H., and Poppenberger, B. (2013). Brassinosteroid-regulated GSK3/Shaggy-like kinases phosphorylate mitogen-activated protein (MAP) kinase kinases, which control stomata development in *Arabidopsis thaliana*. J. Biol. Chem. **288**, 7519–7527.

Kovtun, Y., Chiu, W.L., Tena, G., and Sheen, J. (2000). Functional analysis of oxidative stress-activated mitogen-activated protein kinase cascade in plants. PNAS. **97**, 2940–2945.

Kovtun, Y., Chiu, W.L., Zeng, W., and Sheen, J. (1998). Suppression of auxin signal transduction by a MAPK cascade in higher plants. Nature. **395**, 716–720.

Lampard, G.R., Lukowitz, W., Ellis, B.E., and Bergmann, D.C. (2009). Novel and expanded roles for MAPK signaling in *Arabidopsis* stomatal cell fate revealed by cell type-specific manipulations. Plant Cell. **21**, 3506–3517.

Lampard, G.R., Macalister, C.A., and Bergmann, D.C. (2008). *Arabidopsis* stomatal initiation is controlled by MAPK-mediated regulation of the bHLH SPEECHLESS. Science. **322**, 1113–1116.

Lee, J.S., Huh, K.W., Bhargava, A., and Ellis, B.E. (2008). Comprehensive analysis of protein–protein interactions between *Arabidopsis* MAPKs and MAPK kinases helps define potential MAPK signalling modules. Plant Signaling & Behavior. **3**, 1037–1041.

Limmongkon, A., Giuliani, C., Valenta, R., Mittermann, I., Heberle-Bors, E., and Wilson, C. (2004). MAP kinase phosphorylation of plant profilin. Biochem Biophys Res Commun. **324**:382–386.

Lin, M.K., Belanger, H., Lee, Y.J., Varkonyi-Gasic, E., Taoka, K., Miura, E., Xoconostle-Cazares, B., Gendler, K., Jorgensen, R.A., Phinney, B., et al. (2007). FLOWERING LOCUS T protein may act as the long-distance florigenic signal in the cucurbits. Plant Cell. **19:**1488–1506.

Lincoln, C., Britton, J.H., and Estelle, M. (1990). Growth and development of the axr1 mutants of *Arabidopsis*. Plant Cell. **2**, 1071–1080.

Liu, C., Xu, Z., and Chua, N.H. (1993). Auxin polar transport is essential for the establishment of bilateral symmetry during early plant embryogenesis. Plant Cell. **5**, 621–630.

Lu, C., Han, M.H., Guevara-Garcia, A., and Fedoroff, N.V. (2002). Mitogen-activated protein kinase signaling in postgermination arrest of development by abscisic acid. PNAS. **99**, 15812–15817.

Lukowitz, W., Roeder, A., Parmenter, D., and Somerville, C. (2004). A MAPKK kinase gene regulates extra-embryonic cell fate in *Arabidopsis*. Cell. **116**, 109–119.

Marchant, A., Kargul, J., May, S.T., Muller, P., Delbarre, A., Perrot-Rechenmann, C., and Bennett, M.J. (1999). AUX1 regulates root gravitropism in *Arabidopsis* by facilitating auxin uptake within root apical tissues. EMBO J. **18**, 2066–2073.

Mattsson, J., Ckurshumova, W., and Berleth, T. (2003). Auxin signaling in *Arabidopsis* leaf vascular development. Plant Physiol. **131**, 1327–1339.

Mattsson, J., Sung, Z.R., and Berleth, T. (1999). Responses of plant vascular systems to auxin transport inhibition. Development. **126**, 2979–2991.

Meng, X., Wang, H., He, Y., Liu, Y., Walker, J.C., Torii, K.U., and Zhang, S. (2012). A MAPK cascade downstream of ERECTA receptor-like protein kinase regulates *Arabidopsis* inflorescence architecture by promoting localized cell proliferation. Plant Cell. **24**, 4948–4960.

Miles, G.P., Samuel, M.A., Zhang, Y., and Ellis, B.E. (2005). RNA interference-based (RNAi) suppression of AtMPK6, an *Arabidopsis* mitogen-activated protein kinase, results in hypersensitivity to ozone and misregulation of AtMPK3. Environ. Pollut. **138**, 230–237.

Murphy, A., Peer, W.A., and Taiz, L. (2000). Regulation of auxin transport by aminopeptidases and endogenous flavonoids. Planta. **211**, 315–324.

Nishihama, R., Ishikawa, M., Araki, S., Soyano, T., Asada, T., and Machida, Y. (2001). The NPK1 mitogen-activated protein kinase kinase kinase is a regulator of cell-plate formation in plant cytokinesis. Genes Dev. **15**, 352–363.

Popescu, S.C., Popescu, G.V., Bachan, S., Zhang, Z., Gerstein, M., Snyder, M., and Dinesh-Kumar, S.P. (2009). MAPK target networks in *Arabidopsis thaliana* revealed using functional protein microarrays. Genes Dev. **23**, 80–92.

Reinhardt, D., Mandel, T., and Kuhlemeier, C. (2000). Auxin regulates the initiation and radial position of plant lateral organs. Plant Cell. **12**, 507–518.

Rentel, M.C., Lecourieux, D., Ouaked, F., Usher, S.L., Petersen, L., Okamoto, H., Knight, H., Peck, S.C., Grierson, C.S., Hirt, H., et al. (2004). OXI1 kinase is necessary for oxidative burst-mediated signalling in *Arabidopsis*. Nature. **427**, 858–861.

Robles, P., Fleury, D., Candela, H., Cnops, G., Alonso-Peral, M.M., Anami, S., Falcone, A., Caldana, C., Willmitzer, L., Ponce, M.R., et al. (2010). The RON1/FRY1/SAL1 gene is required for leaf morphogenesis and venation patterning in *Arabidopsis*. Plant Physiol. **152**, 1357–1372.

Rodriguez, M.C., Petersen, M., and Mundy, J. (2010). Mitogen-activated protein kinase signaling in plants. Annu. Rev. Plant Biol. **61**, 621–649.

Ruegger, M., Dewey, E., Hobbie, L., Brown, D., Bernasconi, P., Turner, J., Muday, G., and Estelle, M. (1997). Reduced naphthylphthalamic acid binding in the tir3 mutant of *Arabidopsis* is associated with a reduction in polar auxin transport and diverse morphological defects. Plant Cell. **9**, 745–757.

Sabatini, S., Beis, D., Wolkenfelt, H., Murfett, J., Guilfoyle, T., Malamy, J., Benfey, P., Leyser, O., Bechtold, N., Weisbeek, P.,

et al. (1999). An auxin-dependent distal organizer of pattern and polarity in the *Arabidopsis* root. Cell. **99**, 463–472.

Sachs, T. (1991). Cell polarity and tissue patterning in plants. Development. **113**, 83–93.

Sachs, T. (2000). Integrating cellular and organismic aspects of vascular differentiation. Plant Cell Physiol. **41**, 649–656.

Scarpella, E., Marcos, D., Friml, J., and Berleth, T. (2006). Control of leaf vascular patterning by polar auxin transport. Genes Dev. **20**, 1015–1027.

Scheres, B., and Xu, J. (2006). Polar auxin transport and patterning: grow with the flow. Genes Dev. **20**, 922–926.

Sieburth, L.E. (1999). Auxin is required for leaf vein pattern in *Arabidopsis*. Plant Physiol. **121**, 1179–1190.

Steinmann, T., Geldner, N., Grebe, M., Mangold, S., Jackson, C.L., Paris, S., Galweiler, L., Palme, K., and Jurgens, G. (1999). Coordinated polar localization of auxin efflux carrier PIN1 by GNOM ARF GEF. Science. **286**, 316–318.

Steynen, Q.J., and Schultz, E.A. (2003). The FORKED genes are essential for distal vein meeting in *Arabidopsis*. Development. **130**, 4695–4708.

Swarup, R., Friml, J., Marchant, A., Ljung, K., Sandberg, G., Palme, K., and Bennett, M. (2001). Localization of the auxin permease AUX1 suggests two functionally distinct hormone transport pathways operate in the *Arabidopsis* root apex. Genes Dev. **15**, 2648–2653.

Takahashi, F., Yoshida, R., Ichimura, K., Mizoguchi, T., Seo, S., Yonezawa, M., Maruyama, K., Yamaguchi-Shinozaki, K., and Shinozaki, K. (2007). The mitogen-activated protein kinase cascade MKK3–MPK6 is an important part of the jasmonate signal transduction pathway in *Arabidopsis*. Plant Cell. **19**, 805–818.

Teige, M., Scheikl, E., Eulgem, T., Doczi, R., Ichimura, K., Shinozaki, K., Dangl, J.L., and Hirt, H. (2004). The MKK2 pathway mediates cold and salt stress signaling in *Arabidopsis*. Mol. Cell. **15**, 141–152.

Tsugeki, R., Ditengou, F.A., Sumi, Y., Teale, W., Palme, K., and Okada, K. (2009). NO VEIN mediates auxin-dependent specification and patterning in the *Arabidopsis* embryo, shoot, and root. Plant Cell. **21**, 3133–3151.

Vojtek, A.B., Hollenberg, S.M., and Cooper, J.A. (1993). Mammalian Ras interacts directly with the serine/threonine kinase Raf. *Cell*. **74**, 205–214.

Wang, H., Ngwenyama, N., Liu, Y., Walker, J.C., and Zhang, S. (2007). Stomatal development and patterning are regulated by environmentally responsive mitogen-activated protein kinases in *Arabidopsis*. Plant Cell. **19**, 63–73.

Weigel, D., Ahn, J.H., Blázquez, M.A., Borevitz, J.O., Christensen, S.K., Fankhauser, C., Ferrándiz, C., Kardailsky, I., Malancharuvil, E.J., Neff, M.M., et al. (2000). Activation tagging in Arabidopsis. *Plant Physiol.* **122**, 1003–1013.

Wenzel, C.L., Schuetz, M., Yu, Q., and Mattsson, J. (2007). Dynamics of MONOPTEROS and PIN-FORMED1 expression during leaf vein pattern formation in *Arabidopsis thaliana*. Plant J. **49**, 387–398.

Wilson, C., Voronin, V., Touraev, A., Vicente, O., and Heberle-Bors, E. (1997). A developmentally regulated MAP kinase activated by hydration in tobacco pollen. Plant Cell. **9**, 2093–2100.

Winter, D., Vinegar, B., Nahal, H., Ammar, R., Wilson, G.V., and Provart, N.J. (2007). An 'electronic fluorescent pictograph' browser for exploring and analyzing large-scale biological data sets. PloS One. **2**, e718.